reef quantities about R2,00 per point.

5.4.2 Accuracy

In order to show that the final accuracy is satisfactory, for practical purposes, the theoretical convergence and stress distributions across the central portion of long mined slits of different widths and their abutments are plotted in Figure 5.7 and the results tabulated in Appendix IX.3. The relative convergence criterion was set at 1%. The table in the appendix shows that the resultant accuracy when these results have passed through the off-reef integrator is between 1% and 2%. In practice it was found that the relative convergence criterion could be raised to 4%, without affecting the off-reef integration overmuch, reducing the number of iterations to less than half. (The results appear more oscillatory, but the integration averages out most of these errors).

5.4.3 A Practical Case Study

A case study was performed and the details published in the paper of Plewman, Deist & Ortlepp. A summary appears below.

The study concerned the No. 2 shaft of Harmony Gold Mine (Pty.) Limited. The reef is at a depth of approximately 5 000 ft. and dips 5° to the West. The shaft has a diameter of 20 ft. in a pillar, of about 1 600 ft. diameter, which was undergoing serious fractures of various sidewalls of tunnels and other cavities during 1967. (See section on Scaling, Figure 5.4). In September, 1968, seismic events to the South caused further serious damage in excavations in the pillar area. All mining in the vicinity of the pillar as well as more distantly was halted.

Because of the serious consequence of the loss of production, the following questions had to be answered rapidly :-

(i) Had sufficient stoping been stopped to ensure no further significant increase in the stress in the pillar?

(ii) Could "barrier" areas be left to shield the pillar from appreciable stress increase while permitting mining beyond the "barriers"?

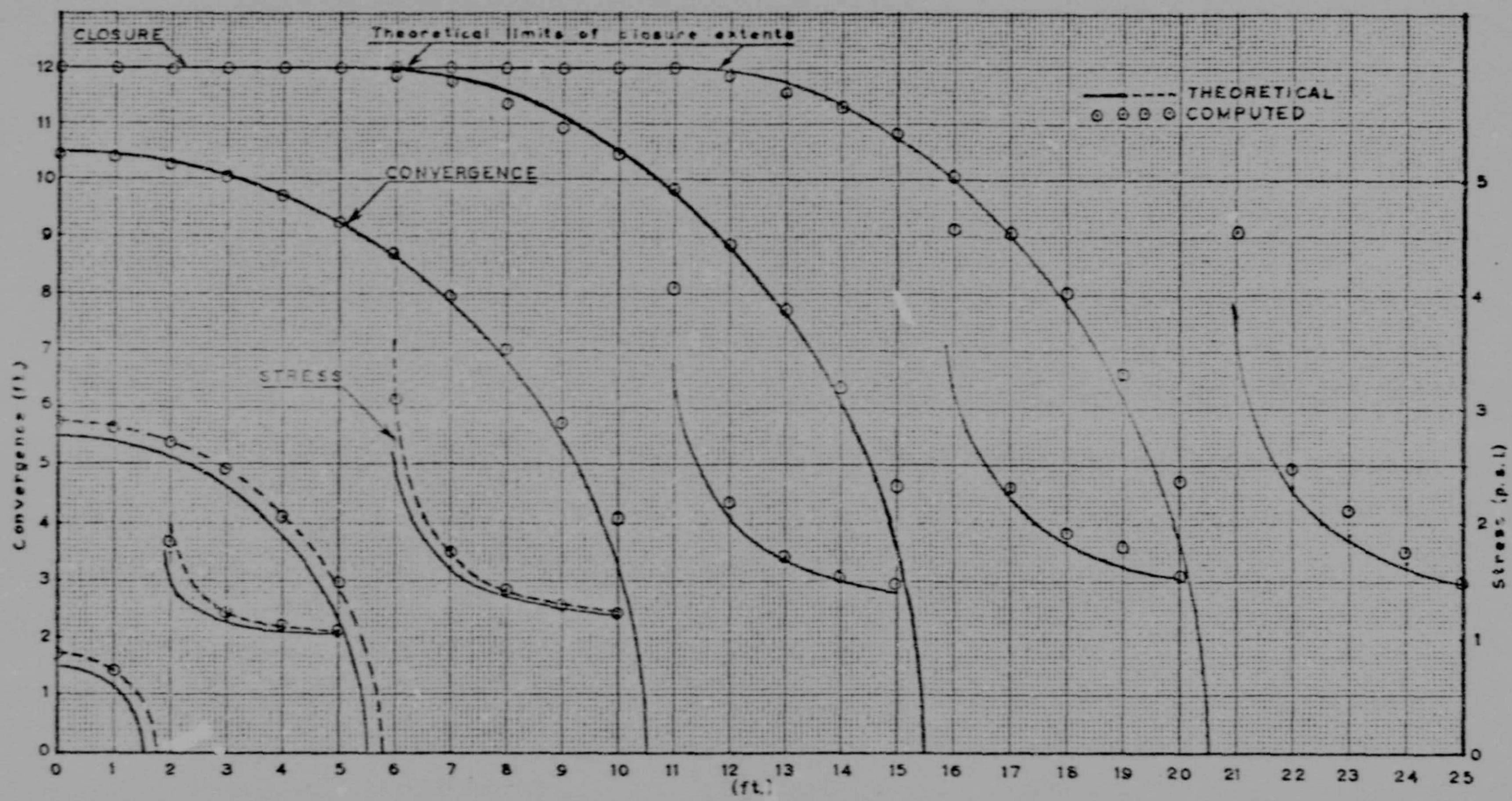

Figure 5.7 Cross-Sectional Distributions of Stress and Convergence for Long Parallel-Sided Slits

(iii) Was it possible to preserve the vital excavation within the pillar area by limited over-stoping in the pillar itself?

(iv) If all the excavations in the pillar had to be abandoned, including the lower portion of the shaft, at what elevation should a transfer system to a new sub-vertical be established?

Ortlepp and Nicoll[9] had shown by measurement that the rock was definitely elastic in this region. No creep was evident at the pillar edge. Thus, the assumptions of the simulation program were satisfied.

As was explained in §5.3.2.3, the scaling feature of MINSIM was used with 75 ft. per unit at the finest scale, which made the shaft pillar approximately 22 MINSIM units in diameter. The coarsest scale was 300 ft. per unit, allowing the stoping information within 8 000 ft. of the pillars to be specified.

The problem was initially solved for the configuration at a stage when damage first became pronounced. At a scale of 150 ft. per unit, the middle scale, successive mining, and replacement of a block in the areas where stoping had been stopped, allowed the changes in stress at points within the pillar to be determined, giving an indication of the importance of this mining to the stress increases in the pillar.

In this way, questions (i) and (ii) could be investigated. In the latter case, the size and location of the "barriers" could be defined such that mining of relatively large blocks beyond the barrier produced negligible stress increases in the pillar.

Similarly overstoping in the pillar, question (iii) could be tested on the finest scale of 75 ft. per unit. Strips of this width were removed to produce a sequence of over-stoping.

Displacements and stresses were computed for points along the shaft axis showing that the horizontal components of differential movements along it were negligibly small, while vertical components were of the order of inches. It was found that the load removed from the haulages as a result of over-stoping was entirely transferred beyond the advancing faces to the remaining segments of the pillar, where it caused a widespread and relatively small increase in vertical stress, and that the stress with increasing height above the pillar decreased rapidly.

5.4.4 Conclusion

The system can be seen to be of great use to the mining industry, espscially in the case of South African mines which are deep and at a shallow angle of dip.

A user manual of the system may be found in Appendix X and a sample run in Appendix XI.

In order to cater for ore bodies with large angles of dip and close to surface, the system had to be extended to the capabilities of MINSIM II to be discussed in Chapters 6 and 7.

CHAPTER 6

THEORY FOR STEEPLY INCLINED REEFS AT FINITE DEPTH

6.1 Introduction

As has been mentioned, the assumption that any influence of the surface can be ignored, has been made so far. This has been justified by various sources [7,18] for the South African gold mining situation.

It was considered necessary to investigate situations where these limitations do not apply. For example, the orebody at Rhokana, Zambia, has an angle of dip $\sim 60^{\circ}$ and extends close to surface. Under these conditions, the rides and shear stresses on the reef plane can become large in comparison with the configurations at small angles of dip. For this reason a more complete analysis is necessary.

Since situations such as Rhokana involve stopes ~ 30 feet, total closure will not be considered here, but may be regarded as a possible extension which may be applied at some later date.

6.2 Boundary Conditions

Since total closure will be neglected, consider the reef divided into an area of excavation, A, and an intact region outside A.

Hence, as before, for the reef in the case of tabular excavations, it is necessary to specify conditions on the hanging- and footwall of the mine opening only [18]. These are that stresses at opposing points on the hanging-and footwalls are approximately equal. Over the intact part of the reef, outside A, the displacement components of the hanging- and footwall are the same, i.e. there is no parting of the seam. Inside A, since the hanging- and footwalls are stress-free, the induced stresses must be equal and opposite to the primitive stresses.

Off the reef, at a sufficient distance below the footwall, the effects of mining become negligible. The plane at infinite depth has zero induced displacements as boundary conditions.

The surface boundary condition is that of being stress-free. Note that both for the surface and for the Zone A, stress-free implies only that three components of stress - the stress normal to the free surface, and the shear stresses in the XZ and YZ planes are zero. The other stress components are not boundary conditions but result from the configuration.

Quantitively, the boundary conditions are as follows :-

For $z = 0$

$$\left.\begin{array}{llll} S_x = 0 & S_y = 0 & S_z = 0 & \text{outside A} \\ \tau_{xz} = -q_{xz} & \tau_{yz} = -q_{yz} & \sigma_z = -q_z & \text{inside A} \end{array}\right\} \quad \text{....(6.1a)}$$

For $z = \infty$

$$u = v = w = 0 \quad \text{...(6.1b)}$$

For $Z = 0$, i.e. on the surface

$$\tau_{XZ} = 0 \qquad \tau_{YZ} = 0 \qquad \sigma_Z = 0 \quad \text{.........................(6.1c)}$$

$$\left.\begin{array}{l} S_x\ (x,y) = u_h\ (x,y) - u_f\ (x,y) \\ S_y\ (x,y) = v_h\ (x,y) - v_f\ (x,y) \\ S_z\ (x,y) = w_h\ (x,y) - w_f\ (x,y) \end{array}\right\} \quad \text{.........................(6.2)}$$

where u, v, w are the displacement components in the x, y, z directions for the hangwall, h, and footwall, f, S_z represents normal closure, and S_x and S_y represent the ride components in the x and y directions respectively. (The ride components are defined as relative displacements of the hanging- and footwall parallel to the plane of the reef).

If the x axis is chosen along strike and the y axis down dip, the primitive stresses given in Cook, et. al., (18), simplify to :-

$$\left.\begin{array}{l} q_z = Q_z \wp \qquad q_{xz} = 0 \qquad q_{yz} = Q_{yz} \wp \\ \text{where} \\ Q_z = -\frac{q}{2}\ ((1+k) + (1-k)\ \mathrm{Cos}\ 2\ \alpha) \\ Q_{yz} = -\frac{q}{2}\ (1-k)\ \mathrm{Sin}\ 2\ \alpha \\ \wp = 1 + \frac{y}{H}\ \mathrm{Sin}\ \alpha \\ \text{and} \\ q = \gamma H \end{array}\right\} \quad \text{...................(6.3)}$$

K = the lateral to vertical primitive stress ratio

α = angle of dip of the reef

H = depth of the reef co-ordinate system origin below the surface

γ = specific weight of rock

The total stresses are the sum of the principal stresses and the stresses induced by mining.

6.3 The Solution

6.3.1 General

The complete elastic differential equations are developed in Appendix XII.

The solution to the problem requires more than three times the computation required by MINSIM I. The general iterative method that has been employed to solve the problem, however, is identical, i.e.

$$\left(\begin{array}{l}\text{Boundary}\\ \text{Conditions}\end{array}\right) = \left(\begin{array}{l}\text{Solutions}\\ \text{in a region}\end{array}\right)_{i+1} + (\text{Kernel}) \cdot \left(\begin{array}{l}\text{Solution}\\ \text{in another region}\end{array}\right)_{i} \qquad \text{..................(6.4)}$$

where i is the iteration count.

The overall picture may be seen by writing the above equation for the overall solution in matrix form, as illustrated in Table 6.1. Note that the kernels have been divided up to show the various types of effects. The mined-to-intact kernels, designated (MI), are derived in Appendix XII (equations XII.28, XII.31, XII.32).

S_z from equation XII.28 has the factor $\frac{1}{\sqrt{x^2+y^2}} \cdot \sigma_z$ applied as in MINSIM I and there are no effects on S_z due to τ_{xz} or τ_{yz}. This kernel $(MI)_{11}$ is thus classed in Table 6.1 as the MINSIM effect kernel for the solution of I_1. It is therefore identical to MINSIM I.

From equations XII.31 and XII.39, $I_2,(S_x)$ has the effect

Table 6.1 Equations of the System

	MINSIM Effect	Poisson Effect	Finite Depth Effect
${}_bI_1 = I_1$	$+(MI)_{11}M_1$	$+ \quad 0$	$+ \quad 0$
${}_bI_2 = I_2$	$+(MI)_{11}M_2$	$+(\overline{MI})_{22}M_2+(\overline{MI})_{23}M_3$	$+ \quad 0$
${}_bI_3 = I_3$	$+(MI)_{11}M_2$	$+(\overline{MI})_{32}M_2+(\overline{MI})_{33}M_3$	$+ \quad 0$
${}_bM_1 = M_1$	$+(IM)_{11}I_1$	$+ \quad 0$	$+(SM)_{11}S_1 + (SM)_{12}S_2 + (SM)_{13}S_3$
${}_bM_2 = M_2$	$+(IM)_{11}I_2$	$+(\overline{IM})_{22}I_2+(\overline{IM})_{23}I_3$	$+(SM)_{21}S_1 + (SM)_{22}S_2 + (SM)_{23}S_3$
${}_bM_3 = M_3$	$+(IM)_{11}I_3$	$+(\overline{IM})_{32}I_2+(\overline{IM})_{33}I_3$	$+(SM)_{31}S_1 + (SM)_{32}S_2 + (SM)_{33}S_3$
${}_bS_1 = S_1$	$+ \quad 0$	$+ \quad 0$	$+(MS)_{11}M_1+(MS)_{12}M_2+(MS)_{13}M_3+(IS)_{11}I_1+(IS)_{12}I_2+(IS)_{13}I_3$
${}_bS_2 = S_2$	$+ \quad 0$	$+ \quad 0$	$+(MS)_{21}M_1+(MS)_{22}M_2+(MS)_{23}M_3+(IS)_{21}I_1+(IS)_{22}I_2+(IS)_{23}I_3$
${}_bS_3 = S_3$	$+ \quad 0$	$+ \quad 0$	$+(MS)_{31}M_1+(MS)_{32}M_2+(MS)_{33}M_3+(IS)_{31}I_1+(IS)_{32}I_2+(IS)_{33}I_3$

Boundary Conditions

${}_bI_1 = {}_bS_z = 0$	${}_bM_1 = {}_b\sigma_z = \propto$ depth	${}_bS_1 = {}_b\sigma_z = 0$
${}_bI_2 = {}_bS_x = 0$	${}_bM_2 = {}_b\tau_{xz} = 0$	${}_bS_2 = {}_b\tau_{xz} = 0$
${}_bI_3 = {}_bS_y = 0$	${}_bM_3 = {}_b\tau_{yz} = \propto$ depth	${}_bS_3 = {}_b\tau_{yz} = 0$

$$\frac{1}{\sqrt{x^2+y^2}} * \tau_{xz}$$ - the MINSIM effect $(MI)_{11}\ I_2$, and

$$\left(\frac{\nu}{1-\nu}\right)\frac{x^2}{(x^2+y^2)^{3/2}} * \tau_{xz}$$ - the POISSON effect, $(\overline{MI})_{22}\ I_2$, and

$$\left(\frac{\nu}{1-\nu}\right)\frac{xy}{(x^2+y^2)^{3/2}} * \tau_{yz}$$ - also the POISSON effect $(\overline{MI})_{23}\ I_3$.

In practice $(\overline{MI})_{22}$ + $(MI)_{11}$ are stored as a common kernel. Similar observations may be made for I_3 --- S_y.

Note that the solutions I_i, i = 1,3 are convergences or rides, which are relative movements of hanging- anf footwall halves of the reef plane along the plane of symmetry, z = 0. The solutions on the surface are those of stress effects needed to create zero surface boundary stress. Although these stresses can have an effect on tha displacements on the reef plane, the effects above and below the plane of symmetry, z = 0, must be in the same direction. Thus, there is no relative movement of floor and roof points due to surface effects. So, in Table 6.1, the finite depth effect is zero.

For the mined out area, the solutions M_i, i = 1,3, similar observations can be made except for surface effect. The MINSIM effect using kernel $(IM)_{11}$ has the factor $\frac{1}{(x^2+y^2)^{3/2}}$, as seen in equations (XII.11), and (XII.14) in Ap··ndix XII, applying to I_1, I_2 and I_3 - the stress solutions σz, τxz, τyz as a result of applied convergences and rides S_z, S_x and S_y.

In addition, I_2 has the factors from equations XII.14, and XII.15,

$$\nu\ \frac{2y^2 - x^2}{(x^2+y^2)^{5/2}}\ S_x + \frac{3\nu\ \ xy}{(x^2+y^2)^{5/2}}\ S_y$$

the kernels $(\overline{IM})_{22}$ and $(\overline{IM})_{23}$, which form the POISSON effect. Similarly for $(\overline{IM})_{33}$ and $(\overline{IM})_{32}$.

Since the stress solutions on the surface, S_1, S_2, S_3 -- σ_Z, τ_{XZ}, τ_{YZ} have an effect on the stresses on the reef plane, these effects, $(SM)_{ij} S_i$, are shown in the table.

On the surface, the reef stress solutions in the mined areas and the reef convergence solutions in the intact areas each have an effect. This will be discussed later.

The full kernels may be found in Appendix XIII.

The system of equations given in Table 6.1 may be represented in a condensed form as :-

$$\left.\begin{aligned} {}_bI_i &= I_i + (MI)\,M_i + (MI)_i M \\ {}_bM_i &= M_i + (IM)\,I_i + (IM)_i\, I + (SM)_i S \\ {}_bS_i &= S_i + 0 + 0 + (MS)_i\, M + (IS)_i\, I, \end{aligned}\right\} i = 1,2,3 \qquad \ldots\ldots\ldots\ldots(6.5)$$

where $(MI) = MI_{ii}$, $(IM) = IM_{ii}$ $\quad (\ )_i$ = cross effect kernels

and $M = \begin{pmatrix} M_1 \\ M_2 \\ M_3 \end{pmatrix}$, $I = \begin{pmatrix} I_1 \\ I_2 \\ I_3 \end{pmatrix}$, and $S = \begin{pmatrix} S_1 \\ S_2 \\ S_2 \end{pmatrix}$

The general iterative scheme may then be written as :-

$$\left.\begin{aligned} I_i^{(n+1)} &= \frac{1}{1+\alpha}\left(\alpha I_i^{(n)} + {}_bI_i - (MI)M_i^{(n)} - (MI)_i M^{(n)}\right) \\ M_i^{(n+1)} &= \frac{1}{1+\beta}\left(\beta M_i^{(n)} + {}_bM_i - (IM)I_i^{(n+1)} - (IM)_i I^{(n+1)} - (SM)_i S^{(m)}\right) \\ S_i^{(m+1)} &= \frac{1}{1+\gamma}\left(\gamma S_i^{(m)} + {}_bS_i - (MS)_i M^{(n+1)} - (IS)_i\, I^{(n+1)}\right) \end{aligned}\right\}$$

$i = 1,2,3$

where n,m are iteration counts, $m \leq n$. $\quad \ldots\ldots\ldots\ldots (6.6)$

6.3.2 The Surface Effect

The surface solutions S_1, S_2, S_3 are those of the stresses, σ_Z, τ_{XZ}, τ_{YZ}. Notice that these have been stated in terms of the surface co-ordinate system, where although there is no angle between the x axis and the X axis, there is an angle of dip between the y- and the Y- axes and the z- and Z- axes, as may be seen from Figure 6.1. Considering the Y-Z plane, as illustrated in Figure 6.2, the σ_z calculated at the surface by the kernels (MS) and (IS) is as shown,

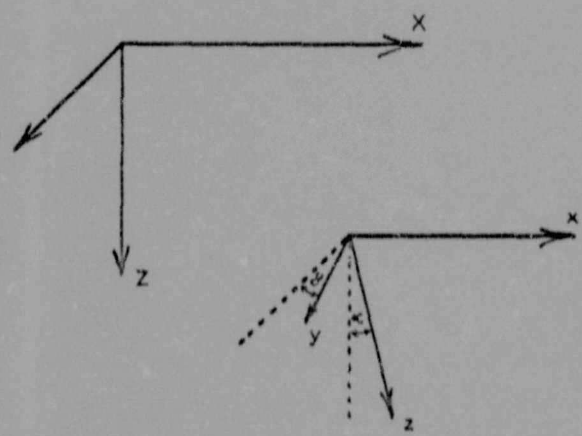

Figure 6.1 Axis Systems

and is not normal to the surface. The normal component is desired since it is the normal stress σ_Z for which there is a known boundary condition. σ_z has a normal component and, in addition, there is a component of σ_y in the Z-direction. Since there is no angle between the x-axes, there is no component of σ_x contributing to σ_Z. The τ_{yz} effect on the surface is also evident.

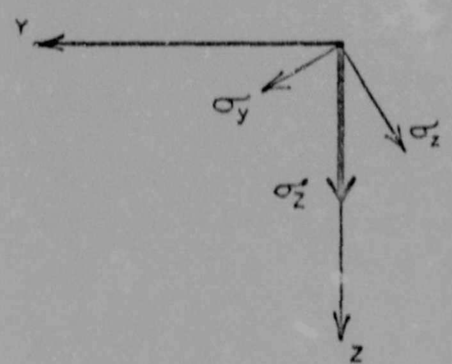

Figure 6.2 σ_z Components

It may be shown, (Appendix XII), that the following holds

$$\left.\begin{aligned}
\sigma_Z &= \sigma_y \operatorname{Sin}^2\theta \;-\; 2\,\tau_{yz}\operatorname{Sin}\theta\operatorname{Cos}\theta \;+\; \sigma_z \operatorname{Cos}^2\theta \\
\tau_{XZ} &= -\tau_{xy}\operatorname{Sin}\theta \;+\; \tau_{xz}\operatorname{Cos}\theta \\
\tau_{YZ} &= \tau_{yz}\,(\operatorname{Cos}^2\theta - \operatorname{Sin}^2\theta) \;+\; (\tau_z - \tau_y)\operatorname{Sin}\theta\operatorname{Cos}\theta
\end{aligned}\right\} \quad \ldots\ldots(6.7)$$

where $\theta = \;\; - \alpha$, the angle of the dip.

A similar transformation is necessary when computing σ_z, τ_{xz}, τ_{yz} from the surface co-ordinate system except that $\theta = +\alpha$, the angle of the dip.

Thus, in order to calculate σ_Z, τ_{XZ}, τ_{YZ}, the quantities σ_y, σ_z, τ_{xy}, τ_{xz}, τ_{yz} need to be evaluated at the surface, and transformed as above, before evaluating S_1, S_2 and S_3. (Table 6.1). Thus, Table 6.1 should be modified for the surface section :-

$$\begin{aligned}
{}_bS_1 &= S_1 + 0 + 0 + \text{transformation} \\
\\
{}_bS_2 &= S_2 + 0 + 0 + \text{transformation} \\
\\
{}_bS_3 &= S_3 + 0 + 0 + \text{transformation}
\end{aligned}
\left\{\begin{aligned}
&(MS)_{11}M_1 + (MS)_{12}M_2 + (MS)_{13}M_3 + (IS)_{11}I_1 + \ldots \\
&(MS)_{21}M_1 + (MS)_{22}M_2 + (MS)_{23}M_3 + (IS)_{21}I_1 + \ldots \\
&(MS)_{31}M_1 + (MS)_{32}M_2 + (MS)_{33}M_3 + (IS)_{31}I_1 + \ldots \\
&(MS)_{41}M_1 + (MS)_{42}M_2 + (MS)_{43}M_3 + (IS)_{41}I_1 + \ldots \\
&(MS)_{51}M_1 + (MS)_{52}M_2 + (MS)_{53}M_3 + (IS)_{51}I_1 + \ldots
\end{aligned}\right\} \quad (6.8)$$

Similarly, the mined equations in Table 6.1 should be written :-

$$\left.\begin{aligned}
{}_bM_1 &= M_1 + (IM)_{11}I_1 + 0 && + SE_1 \\
{}_bM_2 &= M_2 + (IM)_{11}I_1 + (\overline{IM})_{22}I_2 + (\overline{IM})_{23}I_3 && + SE_2 \\
{}_bM_3 &= M_3 + (IM)_{11}I_1 + (\overline{IM})_{32}I_2 + (\overline{IM})_{33}I_3 && + SE_3
\end{aligned}\right\} \quad \ldots\ldots\ldots\ldots\ldots \quad (6.9)$$

where the surface effects SE_1, SE_2, SE_3, are

$$\begin{aligned}
SE_1 &= \text{transformation} \\
\\
SE_2 &= \text{transformation} \\
\\
SE_3 &= \text{transformation}
\end{aligned}
\left\{\begin{aligned}
&(SM)_{11}S_1 + (SM)_{12}S_2 + (SM)_{13}S_3 \\
&(SM)_{21}S_1 + (SM)_{22}S_2 + (SM)_{23}S_3 \\
&(SM)_{31}S_1 + (SM)_{32}S_2 + (SM)_{33}S_3 \\
&(SM)_{41}S_1 + (SM)_{42}S_2 + (SM)_{43}S_3 \\
&(SM)_{51}S_1 + (SM)_{52}S_2 + (SM)_{53}S_3
\end{aligned}\right\} \quad \ldots\ldots\ldots \quad (6.10)$$

The e kernels are also developed in Appendix XIII.

6.3.3 On-Reef Output Integration

Once the solution has satisfied the convergence criteria the results are, as with MINSIM I, stresses in the mined region and compensation convergences in the intact region. The on-reef solution is then obtained by integrating the stresses in the mined region, as an effect on the relative displacement of each point in the mined region, including the effect of the stress on the point itself. In addition the surface effect on the intact area must be computed. In the intact region, the displacements are integrated to compute the induced stress at each point, including the effect of a displacement on each point affecting its own stress.

Note that a compressive stress on a point causes a displacement in the same direction as compressive stresses on surrounding points on the reef. However, for the intact region, a displacement imposed on a point causes a stress of a sign different to that of similar displacements in surrounding points. T... may be deduced from Figure 6.3.

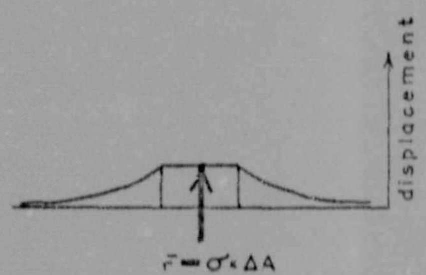

Figure 6.3(a) Displacement Field due to Imposed Stress or Force on an Element

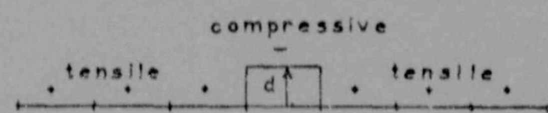

Figure 6.3(b) Stresses caused by Imposed Displacement on an Element

The matrix equations for the on-reef integration then become:-

$$\left.\begin{aligned} I_{i_{output}} &= I_{Vi} - (IM)I_i - (IM)_i I - (IM)_{self} I_i - (SM)_i S \\ M_{i_{output}} &= -(MI)M_i - (MI)_i M - (MI)_{self} M_i \end{aligned}\right\} \quad \text{.....(6.11)}$$

$$i = 1,2,3$$

where,

I_{Vi} = virgin stress, as defined in equations (6.3), and the kernels are as mentioned before, and $(IM)_{self}$ and $(MI)_{self}$ are the reef-effects calculated in Appendix XIII.

6.3.4 Off-Reef Output Integration

Unlike MINSIM I, which needed only the convergences in the mined area to compute the off-reef stresses and displacements, MINSIM II uses the generalized kernels developed in Appendix XII. It includes an integration not only of stresses and convergences in the reef plane, but also the surface effect. The method is an extension of the on-reef output, except that for every point required both stress components and displacement components are computed. (Note that the displacements u, v, w, are computed and not convergences S_x, S_y, S_z).

The internal solutions are convergences in the intact area, counteracting the effect of the stress solutions of the mined area. These stress solutions, combined with the convergence solutions in the intact area and virgin stresses, form a stress-free surface in the mined area. The on-reef calculations were using kernels chosen so that, for z = 0, a zero convergence was produced due to convergence solutions, and zero stresses were produced due to the stress solutions. For z ≠ 0 this is not so. The latter fact is used in the surface iteration, where stresses on the surface were calculated due to the convergence and stress solutions of the reef plane. Similarly, displacement components may also be computed.

Hence, for a general point in space, stresses may be computed as is performed for the effect of the reef on the surface. In addition, the induced displacements (u,v,w) at a general point, may be computed. In general, the surface stress solutions also produce stress and displacements effects on a general point. Note that the displacement component calculation due to reef stresses and displacements depends on whether the general point is above or below the reef plane.

The full point kernels are used. These are summarised in Tables, XII.1, XII.2, XII.3, XII.4, XII.5. The components due to the reef will produce quantities in the reef co-ordinate system. Thus, a transformation of axes, as for the surface calculation, is necessary.

6.4 Conclusion

The mathematical development in this chapter eliminated all approximations assumed in the basic equations of the MINSIM I theory.

Equation (6.6), with the surface solutions modified as in equations (6.8), (6.9) and (6.10), form the basis for a practical solution method. This is implemented in MINSIM II, described in the next chapter.

Since completely general kernels are used for the off-reef integrator, the limitation imposed on the MINSIM I system, i.e. of not allowing the evaluation of points close to the reef, does not apply to MINSIM II. The on-reef quantities are merely a special case of the general off-reef integrator functions.

CHAPTER 7

MINSIM II - IMPLEMENTATION

7.1 Introduction

Many of the techniques used in MINSIM I have been incorporated in MINSIM II. The following points are notable :-

(i) The techniques of grouping points beyond an influence range was handled identically in the two systems. Thus, tables have a level structure, and the lower levels - 1,2,3, after being calculated, have their values rippled up 3-2-1-0 such that level zero has the final result.

(ii) The solution window concept, discussed in §4.2.2 is also incorporated.

(iii) Since the full kernels do not depend only on the distance between the "to" and "from" points, the 8-way symmetry could not be used. However, 4-way symmetry, and an indicator of which quadrant the from-point was in, was incorporated, as will be described in §7.2.3.4.

(iv) Table addressing was also handled in the same way.

(v) The flow of control and the interlocks of certain functions necessary before others is also very similar in the two systems.

(vi) The basic solution flow, apart from the surface iterations and the fact that it applies to the three solutions in place of one, is the same. Updating and scaling phases in which the boundary conditions are modified, as described in §5.3.2.3 are similar except that the surface effects are also incorporated.

Most of this chapter concentrates on the techniques that differ from MINSIM I.

Since the full implementation of MINSIM II is a long-term project, a distinction will be made between phases completed to date and sections still to be implemented. At this stage, a solution incorporating the finite depth effect and arbitrary angles of dip together with update, storage/retrieval and output facilities has been completed. Also, more versatile storage facilities for configurations and solutions are in working order. The scaling feature, the updating window method and the off-reef integrator have yet to be tested. However, since these are, in concept, very similar to MINSIM I, it was not considered necessary to complete these sections for inclusion of the tests into this dissertation.

7.2 MINSIM II - Philosophy

7.2.1 System Philosophy

In Chapter 6, Table 6.1 shows that, for the reef plane iteration alone, there is more than three times as much work to be done in MINSIM II as compared with MINSIM I. For the surface iteration, as may be seen from equation (6.8), an additional five summations are required. Since the core space required for the tables is also increased by a factor of more than 3, many changes in the system philosophy were necessary. The salient points will be brought out here and each point will be discussed in detail in later sections.

Firstly, regarding table space, since it may be shown that the total table area is approximately 1,4 M-bytes, storing all tables in core memory simultaneously is impractical for most available computers. Thus, a paging, virtual storage, concept was designed where the virtual core is a large direct access disk (or drum) file. A service program, DISKIO, is used to fetch, write-out, create space for and free areas of tables on request.

The kernel tables are handled in the same manner. However, since the computation for each kernel table is very complicated, involving many floating point instructions, and since, as will be shown later, there are over 500 kernel tables, each at 4 levels, an attempt is made to keep these tables stored permanently on disk and only re-calculate them if they need to be changed.

On the reef plane, as may be seen from Table 6.1, the effect calculations

$$(\text{effect at to-point}) = \sum_{\substack{\text{Influence}\\ \text{Range}}} (\text{Kernel} * \text{from-point value})$$

for each of the three tables (S_z, σ_z), (S_x, τ_{xz}), (S_y, τ_{yz}) cover the same relative from- and to-points. It was decided not to use the pattern matrix as in MINSIM I. The testing for point-type and the distance table offset computation should not be in the main iteration loop. Hence, influence tables stored on large sequential files were computed. This contained each to-point offset address, followed by a list of kernel table offset addresses, together with the from-point addresses for each kernel offset. This structure is described in detail in Section 7.3.3.4.

Similarly, the surface iteration requires the use of such influence tables five times, as seen from equations 6.8. Hence, the influence tables stored on disk are for $M \rightarrow I$, $I \rightarrow M$, $M \rightarrow S$, $I \rightarrow S$, $S \rightarrow M$ and for the output iteration $S \rightarrow I$.

All input/output is handled by the service program IOCOM. Printer output headings and error messages are stored on a direct access file rather than in each routine requiring the particular output lines. This enables changes to be made to these messages without re-compiling the programs issuing them.

7.2.2 User Philosophy

Experience with the use of MINSIM I led to many improvements being incorporated for the user of MINSIM II.

Input description parameters are entered in the form, KEYWORD=value and many keywords have default values, e.g. DIASZ = 64, POISSON = 0,2, etc. Where parameters must be specified by the user, e.g. ZTOPL, ZSURF, etc. checks are performed and the executation terminated with an error message if the user has failed to do so.

Since error messages and headings are kept in a file, not compiled into the program, their wording can be tailored to suit any particular user. For example, they could be written in a language other than English. The format of many outputs were tidied up, e.g. the on-reef output.

One of the main changes in philosophy is the concept of a "PICTURE" and a "DIAGRAM". A picture is merely the reef mine plan, together with the parameters defining the problem. This picture may be defined to any scale, un-related to the eventual scale of the solution. The maximum size of the picture is the description of an area of 696 x 696 blocks and need not be square.

The description of the picture is by means of a default of either totally mined or totally intact followed, where necessary, by a row-by-row description of the excavation. This can be in the form of a block of points specified by start and end column co-ordinates, or by an "IM" character string.

A diagram for which a solution is to be formed is defined as a square area whose side length is a multiple of 8 blocks. The maximum side is 64 blocks which is the same as the tank-size in MINSIM I.

There is no rim as was the case in MINSIM I. The diagram is defined solely from the picture by specifying the top left diagram co-ordinate position within the picture and a suitable diagram-from-picture scale factor, keyword DPSCALE.

One of the most important aspects of the diagram-picture concept is for updating purposes. For instance, an update may be performed on a diagram solution merely by referring the automatic update function to a new picture and an update list is automatically formed. This is particularly useful when the scale feature is used. A solution of a diagram on a coarse scale is performed, including a large area of the picture. The diagram is scaled up by a linear factor of 2 which causes 4 points to be generated for every one previously, resulting in a very coarse diagram for solution. However, before solution, the scaled problem may be referred to the picture in automatic update mode to refine the boundaries.

The ordinary update mode of the system handles point update as well as character-string and block updates in the same format as was used in creating the picture. In addition, selected keywords can be updated under this operation, thus replacing the MINSIM I "PATCH" verb.

The output verification of a picture or diagram has also been improved compared with MINSIM I facilities. The default is the printing of all keywords and a full picture or diagram. However, the user may choose not to print the keywords or to verify only selected areas of the picture or diagram. In addition, the characters used to represent the intact/mined areas may be chosen by the user at verifying time.